Observations of a Quickly Flapping Interplanetary Magnetic Reconnection Exhaust

Jiemin Wang[1,2] and Yan Zhao[1,2]*

[1]*Institute of Space Physics, Luoyang Normal University, Luoyang, China,* [2]*Henan Key Laboratory of Electromagnetic Transformation and Detection, Luoyang, China*

On the basis of the Petschek reconnection model and the characteristics of reconnection, hundreds of reconnection exhausts were reported in the solar wind. Many multi-spacecraft observations also indicated that interplanetary magnetic reconnection is a quasi–steady-state plasma process and the reconnection X-line can extend hundreds of Earth radii. In this study, we report an interplanetary flapping reconnection exhaust observed by Wind on April 1, 2003 at one AU. The magnetic reconnection event has two adjacent accelerated flows. We compared the plasma and magnetic characteristics of the two accelerated flows and found that the second accelerated flow was due to the back-and-forth movement of the reconnection exhaust. Our observations reveal that not all interplanetary reconnections operate in a quasi–steady-state manner; some reconnection current sheets can move rapidly back and forth.

Keywords: interplanetary magnetic structure, interplanetary current sheet, magnetic reconnection, solar wind, reconnection exhaust

KEY POINTS:

1: A magnetic reconnection event with two adjacent accelerated flows was studied.
2: The detection of the second accelerated flow was due to the back-and-forth movement of the reconnection exhaust.
3: The observations indicate some interplanetary reconnections operate in an unsteady manner with reconnection current sheets flapping rapidly.

INTRODUCTION

Magnetic reconnection is a universal plasma process that not only converts magnetic field energy into plasma kinetic and thermal energies but also breaks and reconnects oppositely directed frozen-in field lines from different plasma regions. This process is implicated in various contexts, including space physics, solar physics, and laboratory plasma physics. The authors in reference [1,2] first established the Sweet–Parker model to describe magnetic reconnection using observations from solar flare activity. One of the model's limitations however is that the reconnection rate is much slower than necessary for flare eruption. In 1964, the authors in reference [3] proposed a new reconnection model and pointed out that the magnetic reconnection is a topological process, and the field lines need not reconnect resistively along the entire length of the boundary layer but could merge over a short length. The key feature of the Petschek model is its assumed separation between the small length scale of the non-ideal electric field, which is
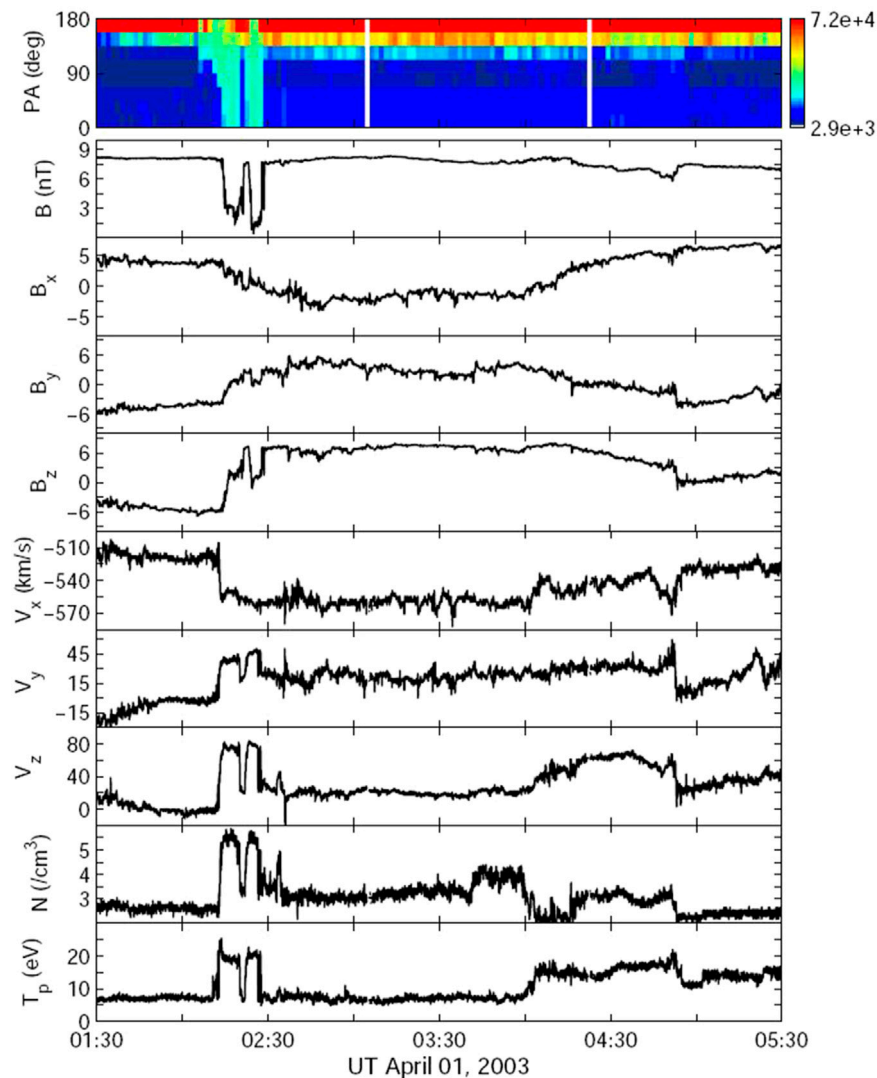
FIGURE 1 | Suprathermal electron pitch angle spectrogram of 165.0 eV, magnetic field, and proton temperature data measured by Wind on April 1, 2003 on the basis of the magnetic reconnection exhaust and the following faster flow.

responsible for breaking magnetic field lines, and the large length scales on which energy is released and dissipated [4]. The Petschek model yields a sufficiently fast reconnection rate by virtue of the localized diffusion region and the extended slow shocks. Reconnection is also characterized by the acceleration of plasma away from the reconnection site in a pair of oppositely directed exhaust regions. The authors in reference [5] proposed a quasi-stationary reconnection exhaust criteria based on the Petschek reconnection model and the characteristic feature of the reconnection process. The requirements to identify reconnection exhausts mainly include 1) a roughly Alfvénic accelerated flow, 2) the enhancements of proton density and temperature, and 3) depression of the magnetic field strength. In accordance with the reconnection exhaust criteria, a large member of observed solar wind reconnection events has been identified and reported (e.g., [5–18]). Multi-spacecraft

observations also indicated that the magnetic reconnections in the solar wind are quasi-steady plasma processes, reconnecting current sheets are roughly planar, and the reconnection X-lines can extend hundreds of Earth radii [6,12,19–21]. Although most reconnection observations revealed that exhausts have quasi-steady, roughly planar structures, several reported exhausts were re-entered one or two times by the same spacecraft after the main exhaust encounter [11,22–26]. Since these re-entry durations were all short, the reported narrow re-entry was interpreted as that exhaust boundaries were non-planar due to their local small-scale folds, even the folds can be orthogonal to the reconnection plane [26]. In addition, the quick flapping of reconnection exhaust may also cause that exhausts were re-entered by one spacecraft. Here, a possible swinging reconnection exhaust observed by Wind on April 1, 2003 was presented.
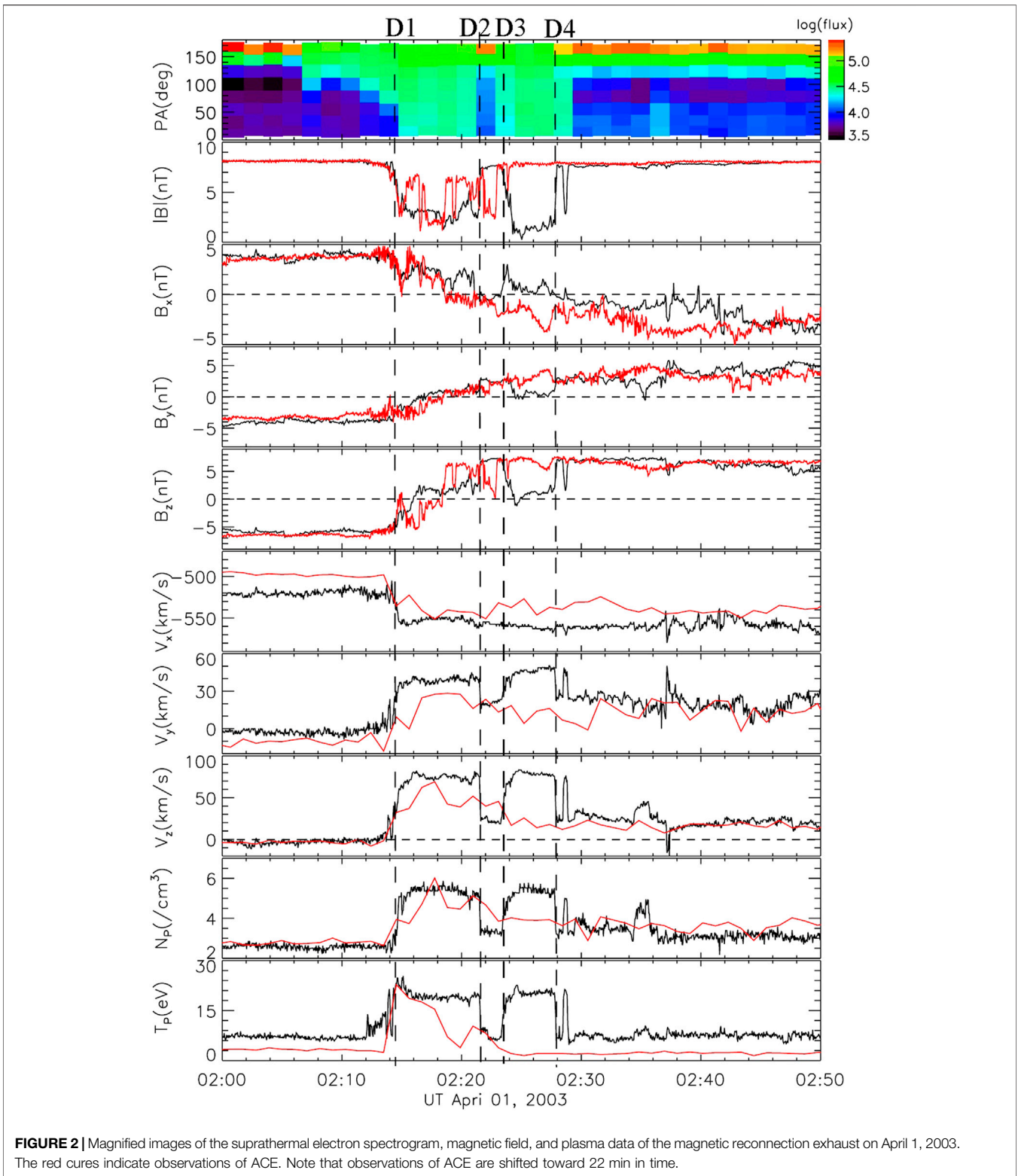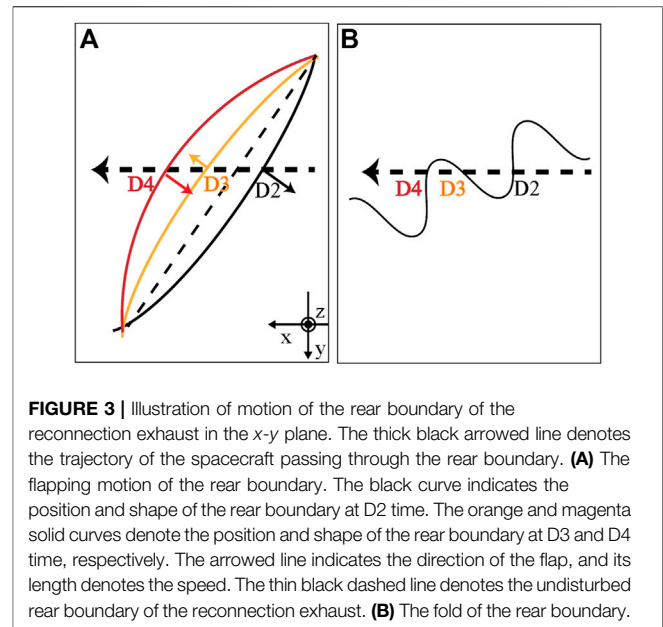
FIGURE 2 | Magnified images of the suprathermal electron spectrogram, magnetic field, and plasma data of the magnetic reconnection exhaust on April 1, 2003. The red cures indicate observations of ACE. Note that observations of ACE are shifted toward 22 min in time.

OBSERVATIONS

Figure 1 illustrates the suprathermal electron pitch angle spectrogram, magnetic field, and plasma data of the magnetic

reconnection event, and the following short, fast magnetic structure, which has been identified as a small flux rope in a small-scale magnetic flux rope database in reference [27], measured by Wind at (228.06, 83.01, 10.58) R_E

(R_E = 6,378 km) in the GSE coordinate system. The top plot displays the suprathermal electron pitch angle spectrograms of 165.0 eV. The subsequent plots show the strength of the magnetic field (B); the x, y, and z components of the magnetic field (B_x, B_y, B_z); the x, y, and z components of the proton speed (V_x, V_y, V_z); proton density (N); and the proton temperature (T_p), respectively. The suprathermal electron data were obtained by using a 3D plasma (3DP) analyzer, and the time resolution was approximately 97 s (Lin et al. 1995). The resolution of the plasma and magnetic field data is 3 s. **Figure 1** also indicates that the magnetic reconnection event occurred at the interface between a faster magnetic structure and its slower frontal background solar wind. The faster magnetic structure lasts less than 3 h, and it exhibits smooth rotations along the magnetic field directions. Similar to a magnetic cloud, the faster magnetic structure may have a closed magnetic configuration because of its smooth field rotations. Magnetic reconnection may occur because of the compression of the following faster closed magnetic structure. **Figure 2** provides the magnified images of the suprathermal electron spectrogram, magnetic field, and plasma curves of the magnetic reconnection event. The authors in reference [13] first identified and reported the magnetic reconnection event, and they also determined the leading boundary of the exhaust at around 02:14:19 UT and found that the duration of the exhaust is 34 min, that is, their identified rear boundary is at around 02:48:19 UT. They also obtained a field shear angle of 153° across the exhaust. **Figure 2** also reveals that the accelerated plasma flow and enhanced proton temperature and proton density regions are mainly at 02:14:19-02:27:52 UT, where the magnetic strength exhibits an apparent depression. In addition, the phase space densities of suprathermal electrons display an apparent enhancement in the region, and these suprathermal electrons may be heated by the reconnection event. In **Figure 2**, it seems that the reconnection event involves two adjacent exhausts, whose boundaries were denoted by four magnetic field directional discontinuities (DDs). The first possible exhaust event is about within 02:14:19-02:21:34 UT, and the second possible exhaust event is from 02:23:31 UT to 02:27:52 UT. Both events have apparent exhaust signatures: the accelerated plasma flow, the enhanced density and temperature, and the depressed magnetic field strength. However, for the first event, the changes between velocity and magnetic field components are correlated with one another at the front boundary of the event and are anticorrelated at the rear boundary, but the changes in velocity and magnetic field are anticorrelated at both sides of the second one. That is to say, only the first event can be identified as a reconnection exhaust according to the reconnection exhaust criteria of Gosling et al. (2005a). Comparing observed features of the two accelerated flow events, we can find that the two events have some similar characteristics. This may indicate that the two accelerated flow events were just one exhaust, which was detected twice in a short time by the Wind spacecraft. As mentioned before, both folds of exhaust boundaries and flapping of reconnection exhausts can cause that exhausts were re-entered by one spacecraft. In the following, we will analyze and discuss the cause of the re-entered reconnection exhaust.

FIGURE 3 | Illustration of motion of the rear boundary of the reconnection exhaust in the x-y plane. The thick black arrowed line denotes the trajectory of the spacecraft passing through the rear boundary. **(A)** The flapping motion of the rear boundary. The black curve indicates the position and shape of the rear boundary at D2 time. The orange and magenta solid curves denote the position and shape of the rear boundary at D3 and D4 time, respectively. The arrowed line indicates the direction of the flap, and its length denotes the speed. The thin black dashed line denotes the undisturbed rear boundary of the reconnection exhaust. **(B)** The fold of the rear boundary.

The spacecraft will detect different signals under different scenarios. For the scenario of flapping reconnection exhaust, the spacecraft detects the rear partial exhaust repeatedly, namely, the spacecraft passes through the same plasma environment twice. Therefore, the observed plasma and magnetic features of the partial re-entered exhaust should be similar to that of the rear part of the main exhaust. In addition, the rear boundary of the main exhaust and the both boundaries of the partial re-entered exhaust should have the same DD, which was crossed three times by the spacecraft. Although the DD moved back and forth with the exhaust, it may keep the roughly planar structure. For the scenario of folds in the rear boundary, the trajectory of the spacecraft should be close to the warping rear boundary so that it can cross its rear boundary more than two times. The spacecraft detects different plasma environments at every turn. Therefore, partial of observed plasma features of two accelerated (or decelerated) plasma flows may be similar, such as proton density and the proton temperature for the two scenarios. But the observations of the magnetic field directions and the proton velocities should be different for the two scenarios [26]. Especially, the rear boundary of the first accelerated flow and both boundaries of the second accelerated flow should be not planar in the fold scenario. The main differences between the two scenarios are illustrated in **Figure 3**.

Now, we examine the two adjacent accelerated flows observed by Wind in more detail. **Figure 2** reveals that the plasma and magnetic characteristics of the two intervals 02:14:19-02:21:34 UT and 02:23:31-02:27:52 UT are approximately consistent, and these characteristics include magnetic field strength, the magnetic field direction, the proton velocity, proton density, and the proton temperature. Especially their profiles of velocity components are almost unanimous. In addition, the profiles of the magnetic field and solar wind speed are symmetric at about 02:22:28 UT. Therefore, we infer that two adjacent accelerated flows only
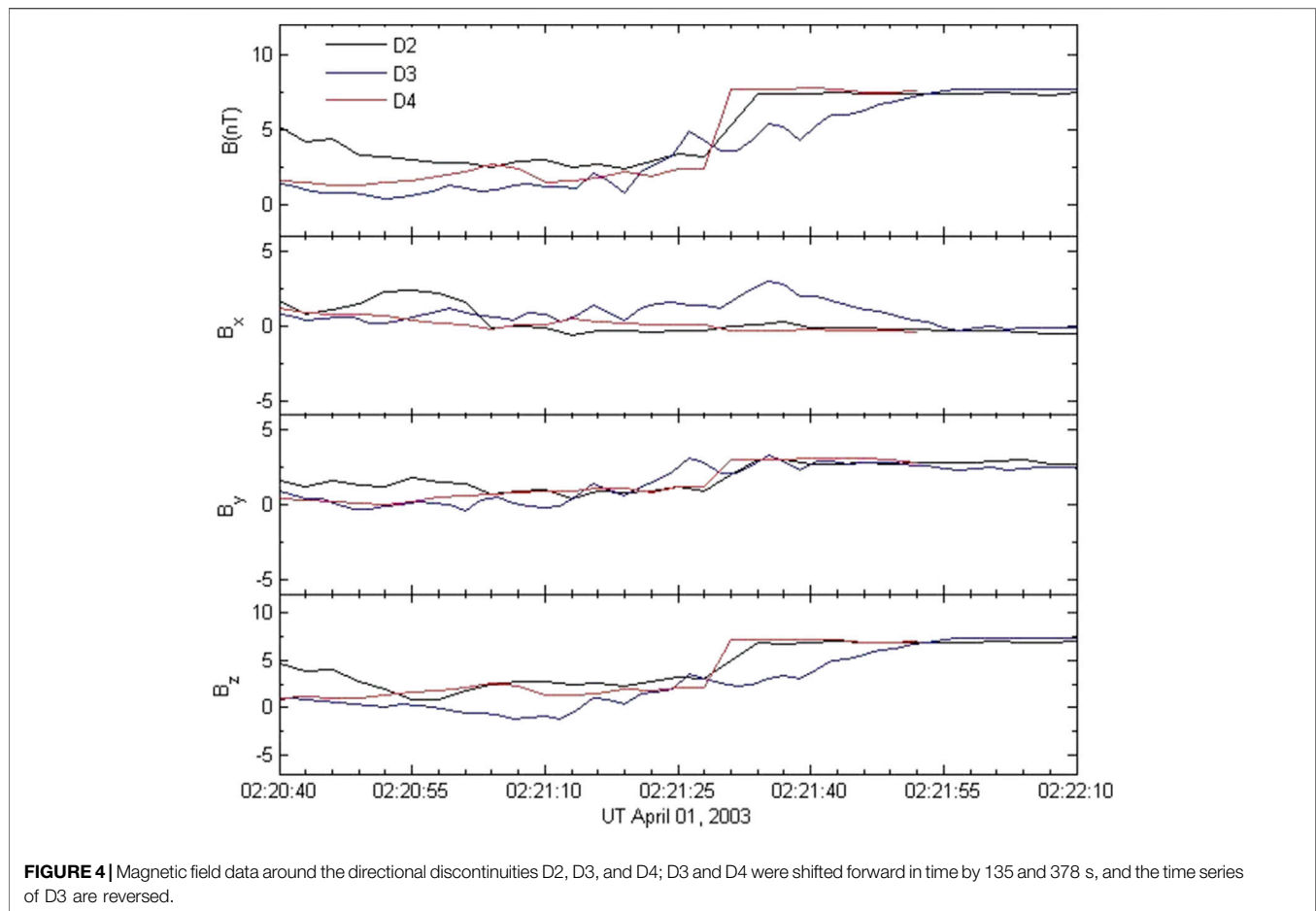
FIGURE 4 | Magnetic field data around the directional discontinuities D2, D3, and D4; D3 and D4 were shifted forward in time by 135 and 378 s, and the time series of D3 are reversed.

TABLE 1 | Normal vectors of the DDs in the GSE coordinate.

	X	Y	Z
D2	−0.611	0.732	−0.301
D3	−0.576	0.750	−0.327
D4	−0.539	0.799	−0.264

represent one exhaust detected twice simply due to its back-and-forth movement. If so, all the directional discontinuities D2, D3, and D4 are the rear boundary of the exhaust, but D3 is crossed by Wind from the outside. All the three directional discontinuities should have consistent variation characteristics. **Figure 4** gives the overlay of time-shifted magnetic field data around the three directional discontinuities. The data of D3 and D4 were shifted forward in time by 135 and 378 s, respectively, the time series of D3 are reversed. **Figure 4** demonstrates that three sets of curves have a similar changing trend, but jump curves of D2 and D4 are steeper than those of D3. This indicates that the Wind spacecraft took more time to cross D3 than to cross D2 and D4. The delayed effect of D3 can be explained with back-and-forth movement of the exhaust. After Wind passed through the rear boundary the first time, flapping reconnection exhaust with the solar wind departs from the Wind satellite quickly. For the second

encounter, the rear boundary needs to come back to scan the Wind satellite. Thus, the second traversing speed must be lower, and correspondingly, its traversing duration was longer. Now that D2, D3, and D4 represent that the rear boundary was crossed at different time, the three DDs should have similar normal directions. A minimum variance analysis (MVA) technique is frequently used to estimate DD normal; here, we also estimated the normals of the three DDs with the MVA technique, and **Table 1** lists their normal vectors in the GSE coordinate. From **Table 1**, one can find that the three normal directions are coincident, and the angles between two of the three normal vectors are in the range of 2.72° and 6.06°. In conclusion, our findings suggest that the reconnection current sheet was quickly moving back and forth when the Wind spacecraft crossed the reconnection exhaust.

SUMMARY AND DISCUSSION

In this study, we report an interplanetary magnetic reconnection event, which was detected by the Wind spacecraft on April 1, 2003. Wind's observations show that the magnetic reconnection event has two discrete accelerated flows, and there is an about 2-min interval between the accelerated flows. The second accelerated flow

indicates that Wind re-entered the main exhaust. But the cause of the re-entered exhaust is different from previously reported re-entered exhaust [11,22–26]. A previous work suggests that the re-entered parts result from the folded local exhaust boundaries. However, the analysis of the reconnection event presented here indicated that the re-entered parts resulted from quickly flapping of reconnection exhaust. The traversing times of D2 and D3 were about 30 and 60˚s, respectively. The speed of the solar wind in the normal direction of the rear boundary was about 313 km/s. Taking this speed as the traversing speed of D2, the traversing speed of D3 should be 156.5 km/s. Such a traversing speed was very likely to be overestimated since D2 was probably moving in a slower speed due to the flapping motion. However, the flapping speed could not be smaller than 313 km/s; otherwise, the observations by spacecraft may not be able to reveal the flapping movement. The duration between D2 and D4 was ~330˚s. Therefore, the amplitude of the flapping motion was at least 16 R_E (taking the flapping speed as 313 km/s). This reconnection exhaust was also detected by ACE at (−5, −29, −65) R_E relative to the position of Wind 22 min later [13]. The observations of ACE are shown in red curves in **Figure 2** (shifted toward 22 min in time for clarity). The rear boundary of the reconnection exhaust at ACE was thought to be at ~02:18:20 (corresponding to a steep and strong change in Bz). Therefore, the duration of the reconnection exhaust at ACE was 260˚s, which was less than that of 450˚s at Wind. The normal direction of the reconnection exhaust was estimated to be (−0.32, −0.93, 0.20) at ACE and (−0.45, −0.85, 0.27) at Wind by applying the hybrid minimum variance analysis [28] method to the whole exhaust. The angle between the two normal was ~8˚. Therefore, the scale of the reconnection exhaust in the normal direction was ~4.5 R_E at ACE and 10.5 R_E at Wind. At ~02:22:50, ACE detected another steep and strong change in Bz. However, it is hard to decide if this steep variation in Bz was caused by re-enter the rear boundary of the reconnection exhaust, due to the low time resolution of the plasma data from ACE. Besides, one can see that the magnetic field was more fluctuating at ACE, which indicates that some explosive event was ongoing. This event may be the cause of the flapping motion of the reconnection current. In conclusion, for many reported reconnection exhausts, their exhaust geometries, the wedge angles, and dimensionless reconnection rates were calculated based on the quasi-stationary reconnection hypothesis (e.g., [28–31]). If reconnection current sheets were flapping when the spacecraft crossed reconnection exhausts, all the estimated values will be unreliable.

DATA AVAILABILITY STATEMENT

Publicly available datasets were analyzed in this study. This data can be found here: http://cdaweb.gsfc.nasa.gov/cdaweb/istp_public/.

AUTHOR CONTRIBUTIONS

JW drafted the manuscript and led the observational analysis. YZ provided heuristic advice and revised the manuscript. All authors contributed to the interpretation of the results and helped draft the manuscript.

ACKNOWLEDGMENTS

REFERENCES

1. Sweet PA. 14. The Neutral point Theory of Solar Flares. *Symp - Int Astron Union* (1958) 6:123–34. doi:10.1017/s0074180900237704

2. Parker EN. Sweet's Mechanism for Merging Magnetic fields in Conducting Fluids. *J Geophys Res* (1957) 62:509–20. doi:10.1029/jz062i004p00509

3. Petschek HE. Magnetic Field Annihilation. In: WN Hess, editor. *The Physics of Solar Flares*. Washington D C: NASA Special Publication (1964). p. 425–39.

4. Longcope DW, and Klimchuk JA. How Gas-Dynamic Flare Models Powered by Petschek Reconnection Differ from Those with Ad Hoc Energy Sources. *ApJ* (2015) 813:131. doi:10.1088/0004-637x/813/2/131

5. Gosling JT, Skoug RM, McComas DJ, and Smith CW. Direct Evidence for Magnetic Reconnection in the Solar Wind Near 1 AU. *J Geophys Res* (2005) 110:A01107. doi:10.1029/2004JA010809

6. Davis MS, Phan TD, Gosling JT, and Skoug RM. Detection of Oppositely Directed Reconnection Jets in a Solar Wind Current Sheet. *Geophys Res Lett* (2006) 33:L19102. doi:10.1029/2006GL026735

7. Feng H, and Wang J. Magnetic-reconnection Exhausts in the Sheath of Magnetic Clouds. *A&A* (2013) 559:A92. doi:10.1051/0004-6361/201322522

8. Feng H, and Wang J. Magnetic Reconnection as a Possible Heating Mechanism of the Local High Temperature Protons within Magnetic Clouds. *Sci China Earth Sci Earth Sci* (2014) 57:1979–85. doi:10.1007/s11430-013-4816-x

9. Gosling JT, Skoug RM, Haggerty DK, and McComas DJ. Absence of Energetic Particle Effects Associated with Magnetic Reconnection Exhausts in the Solar Wind. *Geophys Res Lett* (2005) 32:a–n. doi:10.1029/2005GL023357

10. Gosling JT, Eriksson S, Skoug RM, McComas DJ, and Forsyth RJ. Petschek-Type Reconnection Exhausts in the Solar Wind Well beyond 1 AU:Ulysses. *ApJ* (2006) 644:613–21. doi:10.1086/503544

11. Gosling JT, Eriksson S, Phan TD, Larson DE, Skoug RM, and McComas DJ. Direct Evidence for Prolonged Magnetic Reconnection at a Continuous X-Line within the Heliospheric Current Sheet. *Geophys Res Lett* (2007) 34:L06102. doi:10.1029/2006GL029033

12. Gosling JT, Eriksson S, McComas DJ, Phan TD, and Skoug RM. Multiple Magnetic Reconnection Sites Associated with a Coronal Mass Ejection in the Solar Wind. *J Geophys Res* (2007) 112:a–n. doi:10.1029/2007JA012418

13. Phan TD, Gosling JT, and Davis MS. Prevalence of Extended Reconnection X-Lines in the Solar Wind at 1 AU. *Geophys Res Lett* (2009) 36:L09108. doi:10.1029/2009GL037713

14. Phan TD, Gosling JT, Paschmann G, Pasma C, Drake JF, Øieroset M, et al. THE DEPENDENCE OF MAGNETIC RECONNECTION ON PLASMA β AND MAGNETIC SHEAR: EVIDENCE FROM SOLAR WIND OBSERVATIONS. *ApJ* (2010) 719:L199–L203. doi:10.1088/2041-8205/719/2/l199

15. Feng HQ, Wu DJ, Wang JM, and Chao JW. Magnetic Reconnection Exhausts at the Boundaries of Small Interplanetary Magnetic Flux Ropes. *A&A* (2011) 527:A67. doi:10.1051/0004-6361/201014473

16. Feng H, Zhao Y, Zhao G, Liu Q, and Wu D. Observations on a Series of Merging Magnetic Flux Ropes within an Interplanetary Coronal Mass Ejection. *Geophys Res Lett* (2019) 46:5–10. doi:10.1029/2018GL080063

17. Feng H, Zhao G, and Wang J. Small Interplanetary Magnetic Flux Rope. *Sci China Technol Sci* (2019) 63:183–94. doi:10.1007/s11431-018-9481-1

18. Feng H, Zhao Y, Wang J, Liu Q, and Zhao G. Observations of Magnetic Flux Ropes Opened or Disconnected from the Sun by Magnetic Reconnection in Interplanetary Space. *Front Phys* (2021) 9:679780. doi:10.3389/fphy.2021.679780

19. Phan TD, Gosling JT, Davis MS, Skoug RM, Øieroset M, Lin RP, et al. A Magnetic Reconnection X-Line Extending More Than 390 Earth Radii in the Solar Wind. *Nature* (2006) 439(7073):175–8. doi:10.1038/nature04393

20. Mistry R, Eastwood JP, Phan TD, and Hietala H. Development of Bifurcated Current Sheets in Solar Wind Reconnection Exhausts. *Geophys Res Lett* (2015) 42:513–520. doi:10.1002/2015GL066820

21. Zhao Y, Feng H, Liu Q, and Zhao G. Coalescence of Magnetic Flux Ropes within Interplanetary Coronal Mass Ejections: Multi-Cases Studies. *Front Phys* (2019) 7:151. doi:10.3389/fphy.2019.00151

22. Gosling JT, Eriksson S, Blush LM, Phan TD, Luhmann JG, McComas DJ, et al. Five Spacecraft Observations of Oppositely Directed Exhaust Jets from a Magnetic Reconnection X-Line Extending > 4.26 × 106km in the Solar Wind at 1 AU. *Geophys Res Lett* (2007) 34:L20108. doi:10.1029/2007GL031492

23. Gosling JT. Magnetic Reconnection in the Heliosphere: New Insights from Observations in the Solar Wind. *Universal Heliophysical Process* (2009) 257:367.

24. Lin CC, Feng HQ, Wu DJ, Chao JK, Lee LC, and Lyu LH. Two-spacecraft Observations of an Interplanetary Slow Shock. *J Geophys Res* (2009) 114:a–n. doi:10.1029/2008JA013154

25. Eriksson S, Gosling JT, Phan TD, Blush LM, Simunac KDC, Krauss-Varban D, et al. Asymmetric Shear Flow Effects on Magnetic Field Configuration within Oppositely Directed Solar Wind Reconnection Exhausts. *J Geophys Res* (2009) 114:a–n. doi:10.1029/2008JA013990

26. Mistry R, Eastwood JP, and Hietala H. Detection of Small-scale Folds at a Solar Wind Reconnection Exhaust. *J Geophys Res Space Phys* (2015) 120:30–42. doi:10.1002/2014JA020465

27. Hu Q, Zheng J, Chen Y, le Roux J, and Zhao L. Automated Detection of Small-Scale Magnetic Flux Ropes in the Solar Wind: First Results from the Wind Spacecraft Measurements. *ApJS* (2018) 239(1):12. doi:10.3847/1538-4365/aae57d

28. Gosling JT, and Phan TD. Magnetic Reconnection in the Solar Wind at Current Sheets Associated with Extremely Small Field Shear Angles. *ApJ* (2013) 763(2):L39. doi:10.1088/2041-8205/763/2/l39

29. Xu X, Wei F, and Feng X. Observations of Reconnection Exhausts Associated with Large-Scale Current Sheets within a Complex ICME at 1 AU. *J Geophys Res* (2011) 116:A05105. doi:10.1029/2010JA016159

30. Teh W-L, Sonnerup BUÖ, Hu Q, and Farrugia CJ. Reconstruction of a Large-Scale Reconnection Exhaust Structure in the Solar Wind. *Ann Geophys* (2009) 27:807–22. doi:10.5194/angeo-27-807-2009

31. Lavraud B, Gosling JT, Rouillard AP, Fedorov A, Opitz A, Sauvaud J-A, et al. Observation of a Complex Solar Wind Reconnection Exhaust from Spacecraft Separated by over 1800 R E. *Sol Phys* (2009) 256(1–2):379–92. doi:10.1007/s11207-009-9341-x